Equatorial Solar Tracker Control Using MPPT Technique

Hicham bouzakri *‡, Ahmed Abbou *, Zakaria Abousserhane *, Rafika El Idrissi*

Department of Electrical Engineering, Mohammadia School of Engineers, Mohamed V University in Rabat, Morocco,

(hichambouzakri@research.emi.ac.ma, abbou@emi.ac.ma, zakariaabousserhane@research.emi.ac.ma, rafika.elidrissi@gmail.com)

‡Corresponding Author; Hicham Bouzakri, Tel: +212641652332, hichambouzakri@research.emi.ac.ma

Received: 05.04.2022 Accepted: 26.05.2022

Abstract- To maximize the yield of a photovoltaic panel, a mechanism called a solar follower was introduced. During the day, this gadget permits the panel to follow the sun. The method by which the tracker knows the position of the sun is given either by calculation (Clock or GPS system) or by a sensor (example an LDR sensor), As a result, the solar panel's efficiency is independent of the tracker's movement. We presented a solar follow-up system based on the monitoring of the fluctuation in P_{mpp} power supplied by the PV and managed by an MPPT (Maximum Power Point Tracking) to keep this power at its maximum during tracking correction. The control board activates the tracking motor as it observes the Pmpp power. The moment this power reaches its maximum, the tracking stops. A simulation study has shown us the reliability of this method, and real experience with an equatorial tracker allows us to conclude that this procedure offers great precision with the maximum energy yield extracted.

Keywords MPPT, solar tracker, photovoltaic panel, solar radiation, equatorial mount.

1. Introduction

Morocco has had a national energy policy in place since 2009 to improve energy efficiency through the integration of renewable energies on Moroccan soil. A photovoltaic technology is utilized to create clean energy from solar radiation. With this technology the solar radiation is converted into energy [1-2]. In this way, we tend to place photovoltaic panels perpendicular to direct solar radiation since direct solar irradiation accounts for the bulk of global irradiation [3].

A solar tracker is a gadget that enables a solar panel to follow direct sunlight from dawn to dusk. A lot of research and experiments are being conducted for optimal performance and minimal usage. This study may be classified into two divisions: mono-axial models [4-8] and bi-axial models [9-13].

There are two methods of solar tracking: closed-loop tracking and open-loop tracking. Closed-loop tracking involves using a solar sensor to observe the movement of the sun across the sky, and then the position of the sun is sent to the control board to operate the tracking motors, while open-loop tracking offers purely mathematical calculations, thus making it possible to track the sun without observing it.

Thai researchers have designed a dual-axis solar tracker using a closed-loop tracking approach. The tracking system is designed as an active tracking system based on closed-loop control, using LDR (Light Dependent Resistor) sensors as system inputs. They observed an increase in the energy efficiency of 44.89 percent [14]. The downside of using a simple LDR sensor is decreased tracking accuracy, as LDRs never give exact measurements.

Moroccan researchers have proposed a new tracking method introduced to an azimuthal bi-axial solar tracker. The method consists of extracting the position of the sun in real-time via a camera to activate the two motors, the horizontal motor, and the vertical motor. Experience has shown that the system has a production gain of 32% compared to a fixed installation [15]. They have indeed increased tracking accuracy, but this method will complicate tracking and make the system very expensive.

Other researchers in Greece have developed an azimuthal bi-axial tracker that does not use any solar collector. It is an open control system. They used internal calculations to specify the position of the sun during the day. This system is independent of the state of the sky; it is always running. This is one of the disadvantages of this type of tracking. The prototype has been produced and verified.

The yield of such a system swings between 19.1% and 30.2% depending on the season, with a very small tracking error of only 0.43° [16].

Our first published study is about the modeling and execution of an equatorial mono-axial sun tracker. It's a model based on the notion of pointing the tracking axis towards the pole star because the sun seems to go around it. According to a theoretical and simulation study, we should expect an efficiency of between 91.87% and 100 percent, depending on the season [17].

We then proposed in a second paper that we lower the tipping margin by including a reflection module at the top and bottom of the solar panel. The advantage of this change is that we were able to optimize the yield on solstice days when the yield would have been at a minimum of 91.87% with the original model [18-19].

With a concentrated photovoltaic panel, these two proposed models are invalid. As a result, we proposed a change in a publication to the mechanism entirely to include a second axis known as the tilt axis [20]. All of these models of solar trackers use a simple LDR sensor for tracking. This sensor contains two LDRs separated by a wall. It is a mono-axial sensor since the tracking in these three models uses a single axis.

The goal of this work is to add a new tracking control system to the solar tracker control board, which involves monitoring the power supplied by the PV between the PV and the MPPT (Maximum Power Point Tracking). The tracking motor's orientation is sent by the sun sensor to the control system. Two sensors positioned between the PV and the MPPT will monitor the fluctuation in PV power as the motor turns (current sensor and voltage sensor). The engine will continue to run as long as the power grows, and it will not stop until the power reaches its maximum and begins to decline.

We will start with an explanation of the equatorial solar tracker, which will be used experimentally at the end of the work. After that, we will discuss in detail the proposed method with part of the simulation. Then we will attack the realization part, which begins with the explanation of the proposed flowchart for the solar tracker control board and will end with the implementation of the entire system. Finally, a real experiment will be conducted in order to experimentally value the proposed method.

2. The Equatorial Solar Tracker Model

We all know that the earth's axis of rotation for observers in the northern hemisphere is oriented close to the pole star Polaris. While for those in the southern hemisphere the earth's axis is oriented near Sigma Octantis "Fig.1".

Fig. 1. The orientation of the Earth's axis of rotation.

For that reason all celestial objects in the sky have an apparent motion around Polaris for the northern hemisphere or around Sigma Octantis for the southern hemisphere "Fig.2" and "Fig.3"

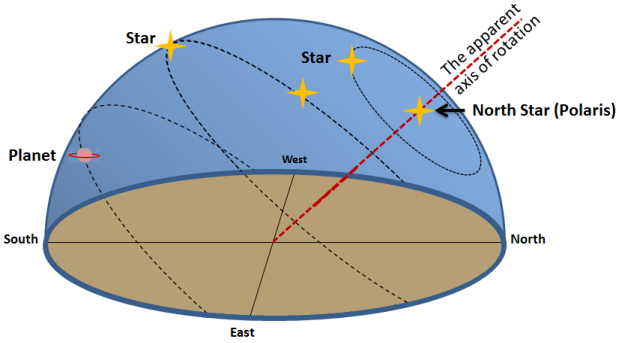

Fig. 2. In the northern hemisphere, objects in the sky seem to revolve around the North star.

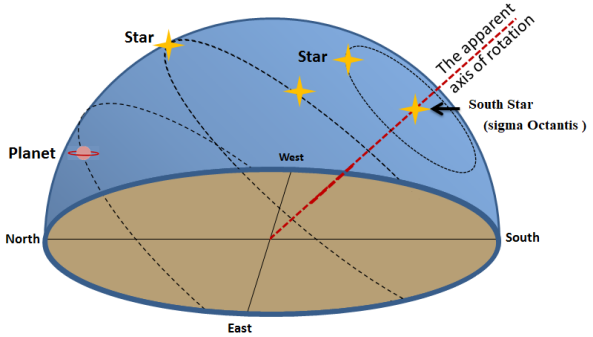

Fig. 3. In the southern hemisphere, sky objects seem to revolve around the star sigma-Octantis.

The sun, it's not exceptional, the sun also has an apparent circular path around Polaris for the northern hemisphere, or around Sigma Octantis for the southern hemisphere. So to get smooth tracking with a single axis of rotation, the tracking axis should be laid facing towards Polaris in the

northern hemisphere "Fig.4" or towards the star Sigma Octantis in the southern hemisphere "Fig.5".

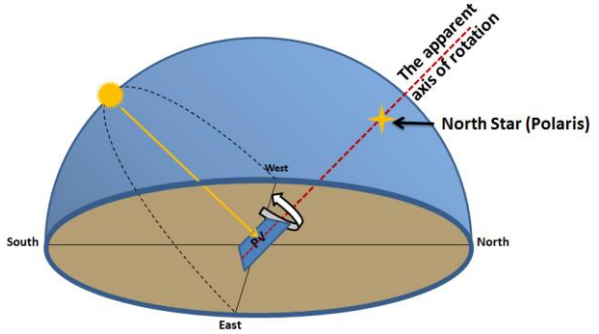

Fig. 4. The solar panel's orientation in the northern hemisphere.

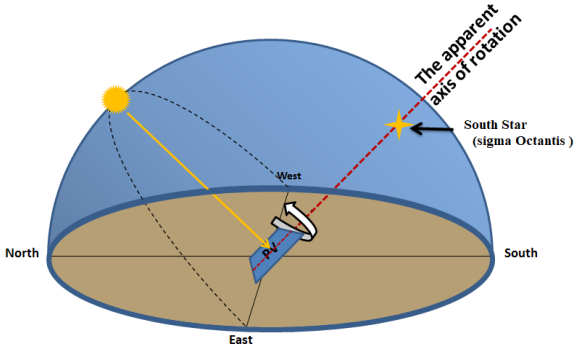

Fig. 5. The orientation of the solar panel in the southern hemisphere.

This apparent path of solar motion is not stable; it changes its inclination between the winter solstice and the summer solstice, passing through the celestial equator at the equinoxes "Fig. 6" [21].

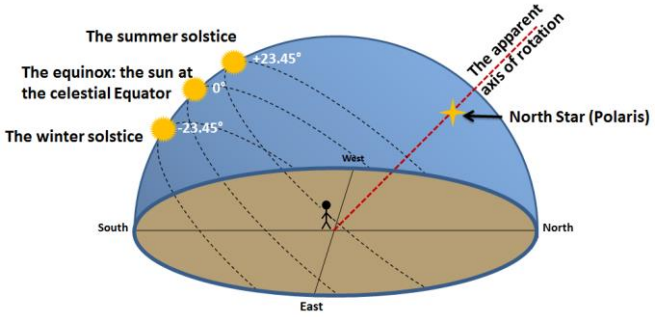

Fig. 6. The annual solar path change.

The daily change in this apparent path follows a sinusoidal relationship, with the celestial equator as the starting point (δ=0°) [21]:

$$\delta = 23.45 \sin\left[\frac{360}{365}(d_n + 284)\right] \text{ in degree} \qquad (1)$$

d_n : From day 1 to 356.

At the summer solstice, we have δ=+23.45°, whereas δ=-23.45° at the winter solstice, but at the equinoxes, we have δ=0°.

To perfectly follow the movement of the solar path in the sky, we'll add an axis called inclination, which will be fixed on the tracking axis as shown in figure 7. This axis will be adapted once at the beginning of the day according to "Eq. (1)" so that it is well oriented towards the solar path on this day. As a result, the suggested solar tracker includes two rotational axes: one of equatorial tracking and the other of tilt correction "Fig.7" and "Fig.8".

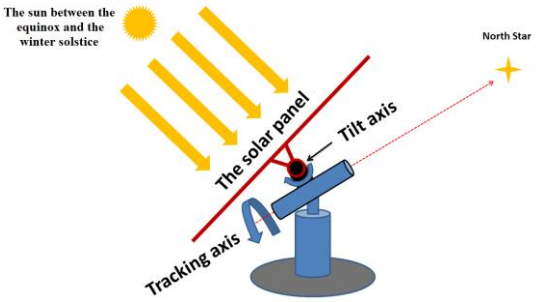

Fig. 7. The tilt axis and the equatorial tracking axis.

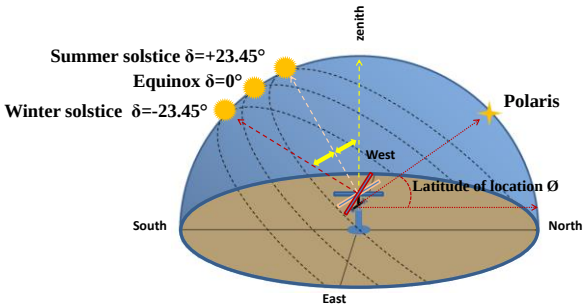

Fig. 8. The tilt axis changes its tilt according to the daily change in solar declination.

3. The Monitoring Logic Proposed

3.1 Tilt Axis

Before sunrise, the solar tracker will be in parking mode, which means, the panel will come face to face with the zenith. This position is important with a view to protect our device from the risks of gusts "Fig.9". To adjust the inclination of the panel, the tilt axis motor needs to moves from the zenith to the apparent solar path for that day, which can be found using "Eq. (1)". Since this manipulation is done only once at the beginning of the day, we will make this manipulation programmed through a clock (closed-loop). The following control system calculates the number of days (d_n) and, according to "Eq. (1)", this system also calculates the angle of a solar inclination concerning the celestial equator, then it calculates the angle between the zenith and the solar path for that day. This angle equals: $\delta' = Ø - \delta$ (Ø is the latitude of place) "Fig.10" [20].

And according to "Eq. (1)", this angle will be:

$$\delta' = Ø - 23.45 \sin\left[\frac{360}{365}(d_n + 284)\right] \text{ in degree} \qquad (2)$$

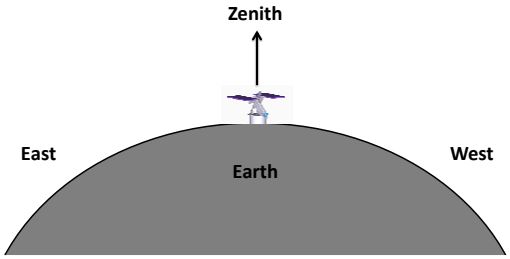

Fig. 9. The solar tracker in parking mode.

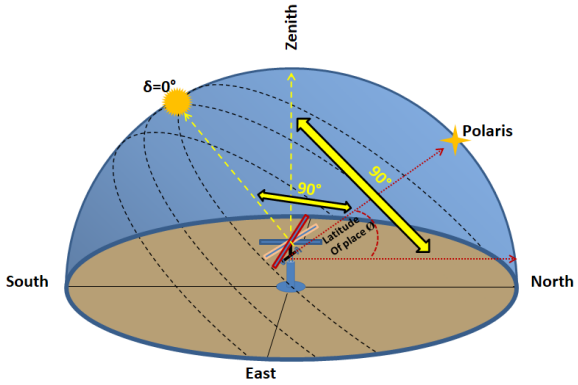

Fig. 10. The difference in orientation between the axes oriented towards the celestial equator and those oriented towards the zenith.

Below "Fig.11" we have a diagram showing the programmed manipulation of the tilt axis.

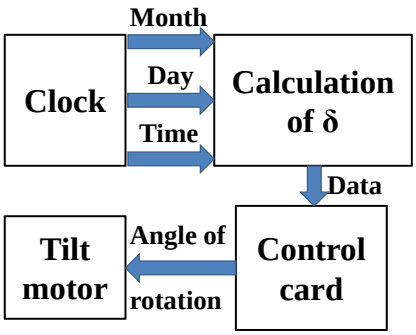

Fig. 11. The daily check of the tilt axis.

3.2 Tracking Axis

Since the manipulation of the tilt axis is done once daily, we have decided that the correction of this axis should be in programmed mode (open loop). The case is different for the tracking axis, which will be in sensor mode (close loop) since the correction is permanent during the day. That is to say, to specify the position of the sun, we will install a solar sensor.

The sensor chosen for this manipulation is a simple sensor with two LDRs connected to a voltage divider circuit, which offers a voltage for each LDR between 0 V and 5 V, which will be converted into binary code later, this process is done via an analog-digital converter of the microcontroller chosen for the control board as illustrated in "Fig.12".

So this sensor provides the control system with the position of the sun during the day. If the 1st LDR is illuminated while the 2nd is under the shadow, it means the sun is located in the east of the panel and the control system operates the tracking motor to the east. If the 1st LDR is under the shadow while the 2nd is illuminated, it means that the sun is west of the panel and therefore the control system operates the tracking motor to the west. The motor only stops if both LDRs are fully illuminated, and therefore, the two sensor output voltages are equal. The choice of this type of sensor is due to the simplicity of production and handling as well as maintenance. However, this doesn't prevent using another sensor that performs the same function [20]. In the case of an overcast sky, the sun is absent, so the two LDR values will be equal. The tracking motor will not be activated as long as its two values are equal "Fig.12".

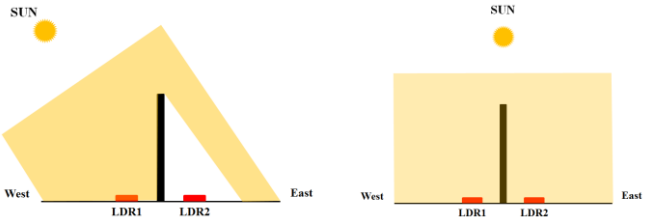

Fig. 12. The sun's position in reference to the two LDR sensors.

Below is a flowchart that shows tracking correction by a dual LDR sensor "Fig.13".

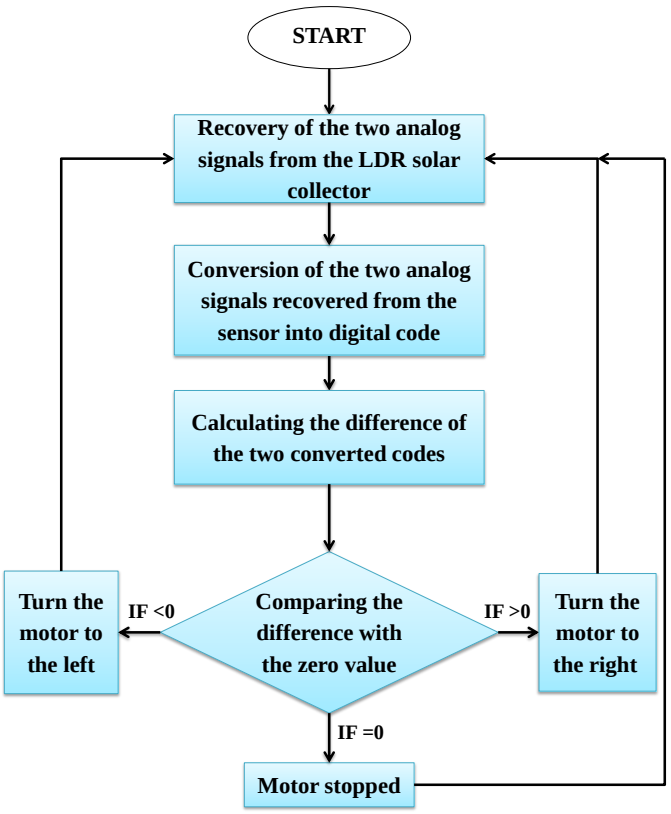

Fig. 13. The flowchart of tracking correction with a dual LDR sensor.

4. Equatorial solar tracker control using MPPT techniques

The MPPT technique is a device added at the output of the photovoltaic panel (PV) whose role is to track the maximum power point of the PV panel. This technique is necessary to extract the maximum power from the PV panel, see "Fig.14" and "Fig.15" [22-23].

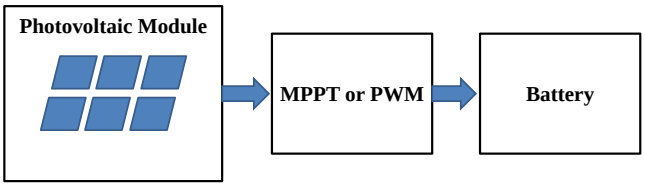

Fig. 14. A PV module is used to charge the batteries using the MPPT technique.

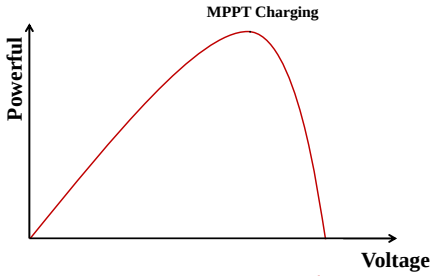

Fig. 15. The Maximum Power Point Tracking.

Even with a high-level sensor, we will never have perfect tracking accuracy, especially with the use of a concentrated PV panel, whose tracking error margin must be almost zero. We also know that the maximum power ($P_{mpp} = V_{mpp} + I_{mpp}$)) is influenced by the amount of solar irradiation, which influences the PV current, and by temperature, which in its turn influences the PV voltage. Consequently, a perfect orientation of the solar panel towards direct solar irradiation does not always mean that we are at the maximum power point, since an increase toward direct solar irradiation will imply an increase in the temperature, and the increase in the temperature consequently will imply a decrease in the voltage.

The idea proposed is to implement the P&O algorithm into the tracking system of the equatorial axis (tracking axis).

We put current and voltage sensors between the PV and the MPPT device to measure, at each instant, the maximum power of the PV panel (Pmpp). This power is controlled, as already mentioned, by the MPPT, and therefore, this assembly requires the presence of an MPPT. The solar tracker control board will process this measured power at the PV panel output. During the tracking correction, we will eliminate the solar collector. The tracking motor rotates from east to west. During its rotation, the system observes the power of the PV panel (Pmpp). If it increases, the motor continues monitoring and only stops if the measured power begins to decrease. Then we are at the point of maximum power, as observed in "Fig.16", "Fig.17" and "Fig.18". The motor continues to turn even if the sensor informs us that it is oriented precisely to direct solar radiation, it only stops if the power reaches its peak.

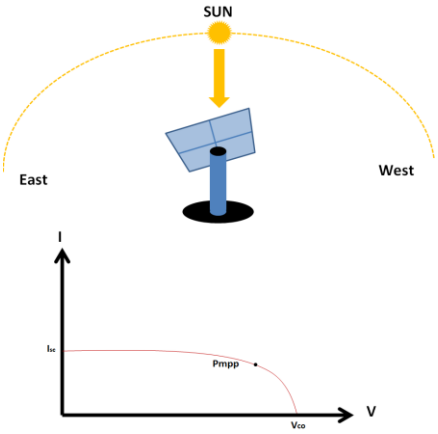

Fig. 16. The power increases as the panel approaches the ideal orientation.

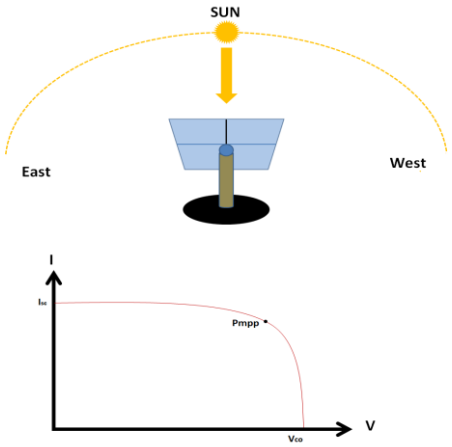

Fig. 17. The power is at its maximum and the panel is at its exact orientation towards the direct solar radiation.

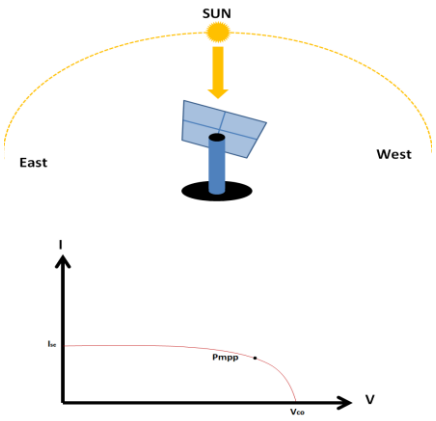

Fig. 18. The power decreases as the panel moves away from the ideal orientation.

5. Simulation

Since the method we are explaining is based on the principle of observing the power supplied by the PV with the use of an MPPT, we will prove by simulation that the best method to have the maximum power of a moving PV is to observe its power Pmpp.

We will use MATLAB version 2018b software for the simulation. We are going to simulate two MPPT techniques. The first one is based on the direct conventional method based on the P&O algorithm [22], and the second one is based on the hybrid method that combines the artificial neural network (ANN) and the backstepping nonlinear controller (ANN-Backstepping) [22]. "Fig.19" and "Fig.20" depict the global schemes of the PV system based on the two mentioned techniques.

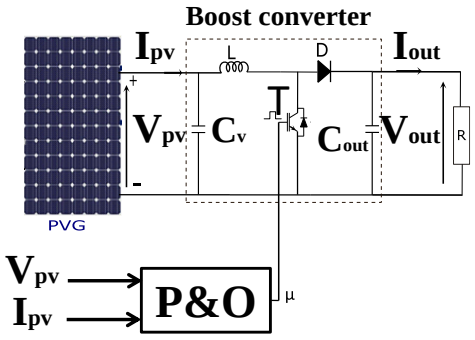

Fig. 19. The Perturb & observe (P&O) technique.

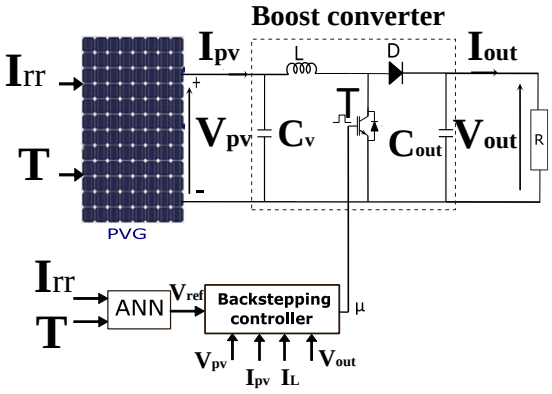

Fig. 20. The ANN-Backstepping technique.

To control the maximum power Pmpp, the P&O controller uses V_{pv} and I_{pv} (the PV voltage and current) sensors, as observed in "Fig.19". The ANN-Backstepping technique is based on two loops. The first one is based on the ANN that provides the optimum voltage corresponding to the maximum power as a reference to the backstepping controller in the second loop. This nonlinear controller compares the reference voltage provided by the ANN with the PV panel voltage by controlling the duty cycle of the boost converter, see "Fig.20". This method makes the controller fast, stable, and more precise.

A solar tracker's tracking correction is a brief procedure in which the PV panel is orientated towards direct sun radiation for a few seconds. In other words, during this period, the solar radiation incident on the panel grows until it reaches its maximum, at which point the PV panel is perpendicular to the direct solar radiation. Regardless of the amount of solar energy or the temperature absorbed by the PV panel, the solar sensor aids the tracker in orienting itself towards the sun. Because the power supplied by the PV panel during tracking correction has to be monitored, this power must be proportional to solar radiation, i.e., the greatest power produced by the PV panel indicates the maximum solar radiation. The simulation consists of introducing into the two controllers for 20 seconds the quantity of variable solar radiation as well as the temperature.

As depicted in "Fig.21" and "Fig.22", in the 5th second, solar radiation rises from 450 W/m2 to 500 W/m2, while the temperature remains constant at 25°. At the 9th second, the temperature goes from 25° to 30° with a constant amount of solar radiation. At the 12th second, the radiation reaches a maximum of 1000 W/m2 with a temperature that also reaches a maximum of 45 °. The solar panel is perpendicular to the direct sun radiation in this position. Finally, the radiation and the temperature go down on the 17th second when the panel moves away from the correct orientation.

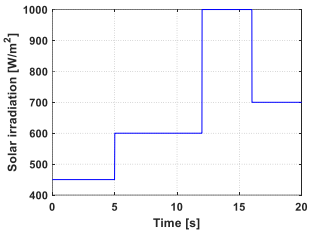

Fig. 21. The variation of solar radiation during the simulation.

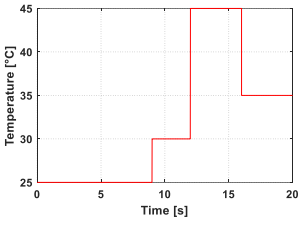

Fig. 22. The temperature variation during the simulation.

"Fig.22" illustrates the results of the evolution of the power Pmpp during this test period of 20 seconds. We can notice that the increase in solar radiation has involved an instantaneous increase in power. With the P&O controller, the curve is more disturbed compared to that of the ANN-Backstepping controller, due to the accuracy of the latter. We can see a small drop in power at the 9th second due to an increase in temperature, but this variation is negligible because the power remains constant until the increase in solar radiation at the 12th second.

Therefore, we can see that the variation of the power Pmpp is identical and proportional to the variation of the solar radiation amount. This allows us to conclude that the best method to observe the evolution of the amount of solar radiation is to observe the power Pmpp provided by the PV panel. We can also notice from "Fig.24" that we can use the current in the observation instead of using the power, since now when the power reaches its peak, the current also reaches its peak. The PIC16F877A used in the realization is a microcontroller that works at 20 MHz, so the control board can quickly detect any variation of P_{mpp} power.

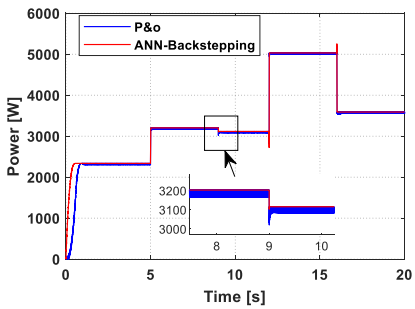

Fig. 23. The variation of the P_{mpp} during the simulation.

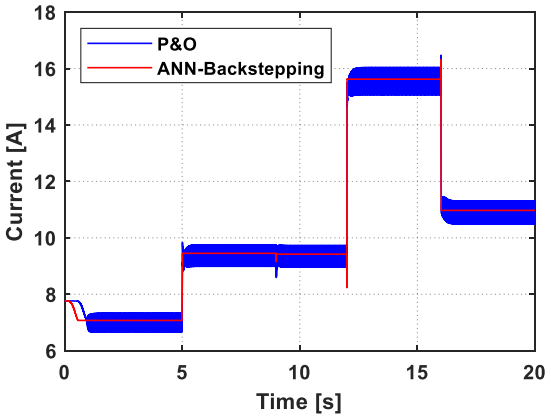

Fig. 24. The variation of the Impp during the simulation.

6. Realization

We'll use the prototype solar tracker depending on the publication [20]. This prototype is an equatorial bi-axial solar tracker which holds the panel and moves it on two axes. It has two motors; one of the tilt axis and the other for equatorial tracking. The sensor used in the prototype is a two-LDR sensor that works as shown in "Fig.12". This solar tracker works exactly as we explained in the previous chapter, i.e., it has an axis of inclination that should be reset repeatedly only once at the beginning of the day to put the panel oriented towards the solar path. The second axis is the equatorial axis, which has the role of monitoring guided by the LDR solar sensor.

We will add to this prototype the MPPT guidance system explained in the previous chapter. For this purpose, we will keep the LDR sensor just to know the state of a cloudy or clear sky, and we will add a current sensor (acs712) and a voltage sensor (DC0–25V input voltage range) between the PV and the MPPT device as shown in "Fig.25".

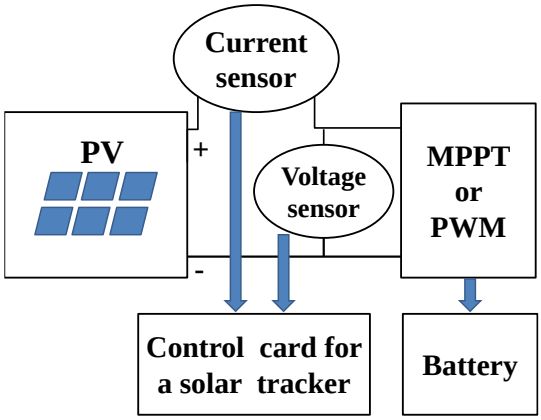

Fig. 25. The instalation of the voltage and current sensors.

The outputs of these sensors will be connected to the solar tracker control board. In this way, the tracker can monitor the instantaneous power supplied by the PV. Below is the complete flowchart proposed for our equatorial tracker with the introduction of the power monitoring system "Fig.26".

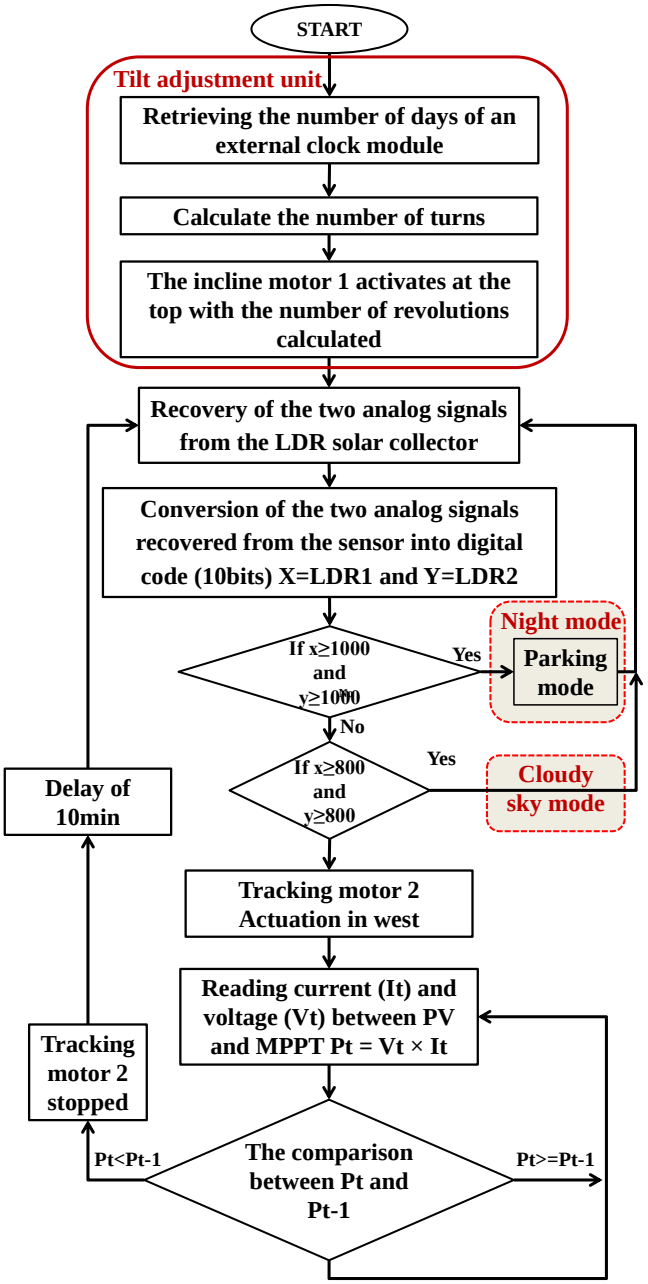

Fig. 26. The control board flowchart.

Through the tilt adjustment unit "Fig.26", the system must put the panel at the proper angle to the sun. Only once a day, at the beginning of the day, is this modification performed. An external clock module provides the system with the current day's number. The system then determines how many spins the tilt motor (motor 1) must make using "Eq. (1)". Finally, the tilt motor 1 is turned on at the top to tilt the panel.

After adjusting the tilt of the panel, the system links the analog inputs from the LDR1 and LDR2 solar collectors, then converts them into 10-bit digital code (between 0 and 1023) and stores them, respectively, on the X and Y variables. Subsequently, we will test these values if they are all greater than 1000 (value per experiment). If yes, that is to say, that the two DLRs are in total darkness, and then we are in night mode. The solar tracker switches to parking mode

"Fig.9". If not, that is to say, we are in day mode. If they are equal and all greater than 800 (the experimental value), i.e. the sky is overcast, the system resets and the tracker enters shutdown mode to conserve power. If the variable of the two LDRs is less than 800 (value per experiment), then we are in a clear sky day mode and will start tracking.

Since the sun during the day makes an apparent course from east to west, the solar tracker control board operates the tracking motor in the west. As the motor rotates, the control board observes the evolution of the power between the PV and the MPPT. The system records the measured power (Pt-1) and observes the power again (Pt) if Pt>=Pt-1 the system continues the observation of the power and the motor continues the follow-up. If Pt<Pt-1 the system stops the tracking engine and goes into standby for 10 minutes. After 10 minutes, the system restarts, reading the LDR sensor again.

Remark: We chose an average standby period of 10 minutes to reduce the consumption of the tracking motor and keep the tracking level almost at the maximum (10 minutes corresponds to an apparent movement of the sun of 2.5°).

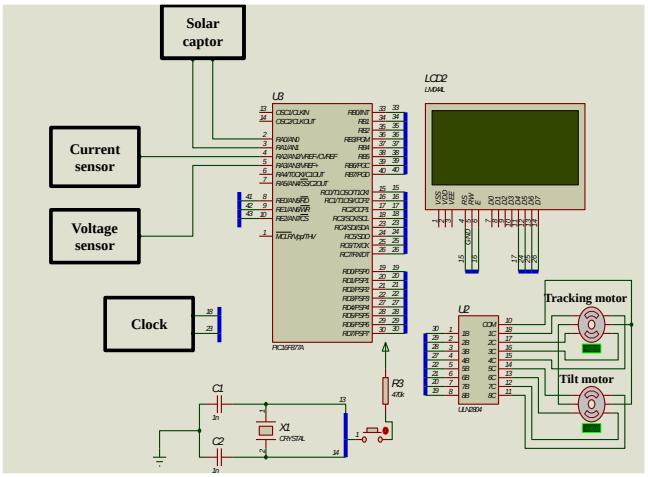

Fig. 27. The schematic of the solar tracker control board.

"Fig.28" and "Fig.29" show the solar tracker used in the experiment with the control system explained in this article.

Fig. 28. The equatorial bi-axial solar tracker used in the experiment.

Fig. 29. The solar tracker control board.

7. Experience and Results

We will move on to real experience to enhance the proposed system. We'll experiment using a bi-axial equatorial solar tracker, as realized and detailed in the publication [20]. And we will add the modification proposed by the flowchart in "Fig.26" and the diagram in "Fig.27" to the main program of the control board.

The experiment consists of making a comparison between two identical photovoltaic panels, one with the equatorial tracker and the other with a fixed installation.

Where Isc is proportional to solar radiation [23-25], both panels will be valued as empty, i.e., we will compare the Isc of the two solar panels. The tracking command only observes the short-circuit current of the panel in equatorial tracking mode. As long as the radiation incident on the photovoltaic panel increases, the Isc also increases, and when we reach the maximum of Isc, it means that we have reached the maximum absorbed solar radiation. At the time, the panel was perfectly oriented toward direct solar radiation.

Before launching the experiment, we will make an experimental analysis of equatorial tracking according to the proposed method, with the observation of the short-circuit current Isc.

An Arduino will show us the current values as the tracking motor is activated "Fig.30". The control card has a display that shows the values of the two LDRs of the solar collector (each value between 0 and 1023) "Fig.31". We are going to compare the variety of the Isc with the variation of the two LDR values.

The characteristics of the photovoltaic panel used: $V_{co} = 22{,}1V$, $V_{mpp} = 18{,}2V$, $I_{sc} = 2{,}95A$, $I_{mpp} = 2{,}75A$

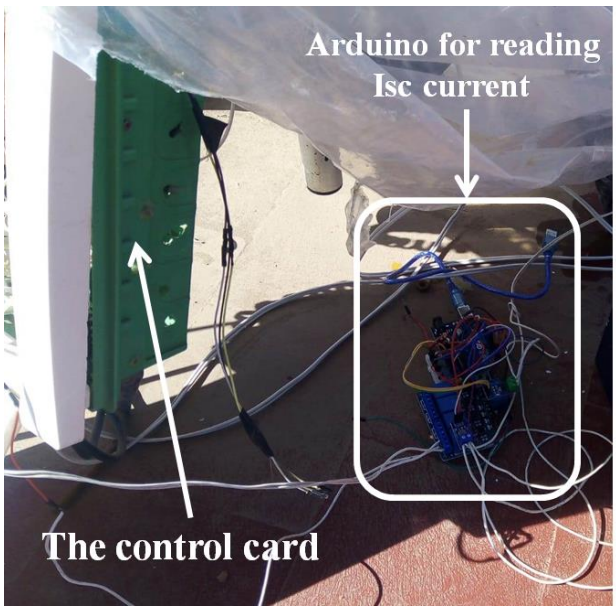

Fig. 30. Arduino displays Isc current on a computer.

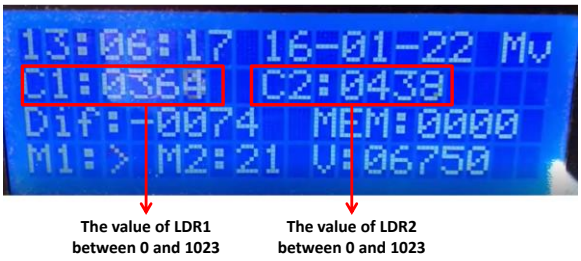

Fig. 31. The LCD on the solar tracker control board.

As shown in "Fig.32", the current increases when the motor is running. At some point, the current stabilizes (the numbers outlined in verse in "Fig.31") and begins to decrease. This is where the motor is stopped. "Fig.33" is a real photo taken from the LCD of the control board and clearly shows us that the peak of Isc does not correspond to the equality of the values of the LDRs of the solar collector. This means that with an ordinary collector, we are far from high precision. Even with an accurate solar sensor, the method we have proposed ensures high tracking accuracy and, therefore, maximum performance.

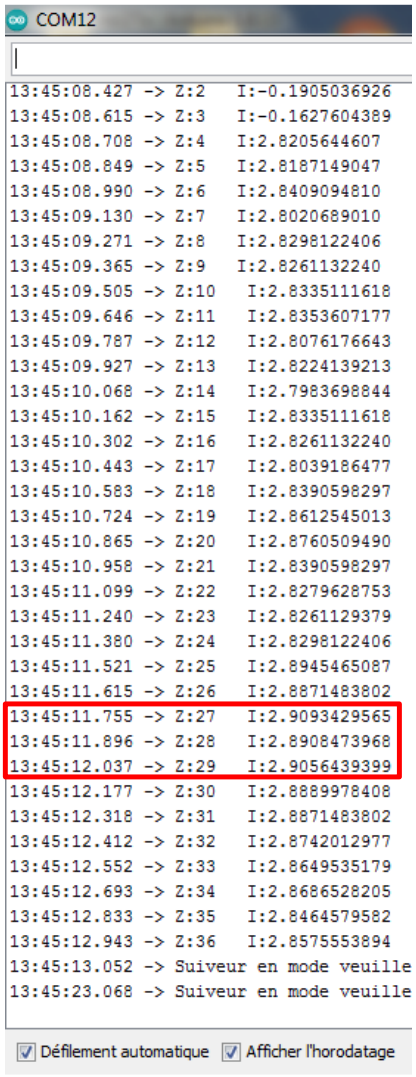

Fig. 32. The values of current Isc are measured at the output of moving PV.

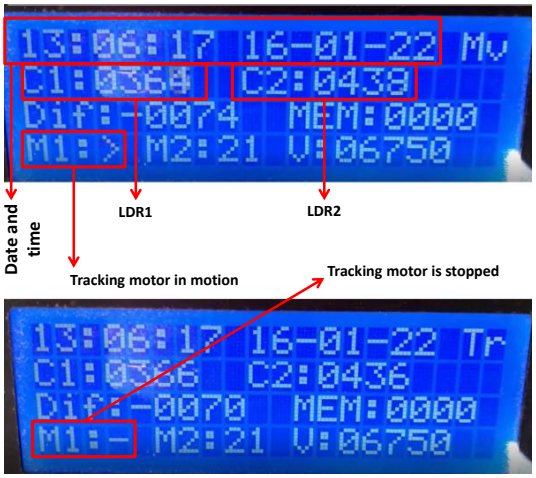

Fig. 33. LCD with the values of LDR1 and LDR2 at the start of the tracking correction and the end of the correction.

Let us now turn to the experience by comparison. The experiment was done on January 27, 2022, from noon to sunset. Table 1 and "Fig.34" show the results of the comparison between the panel in equatorial tracking mode and the panel in fixed mode.

Table 1. Results of the experiment of January 27, 2022.

	PV in solar tracker		Fixed PV	
Hour	**Vco**	**Isc**	**Vco**	**Isc**
13:44	25,002040	3,1590313	24,975158	3,0073692
13:54	25,002040	3,1220400	24,907947	3,0184664
14:05	25,002040	3,0517578	24,997154	2,9888736
14:15	25,002040	3,0406610	24,998376	2,9666790
14:26	24,994709	2,9740772	24,923831	2,8483076
14:39	25,002040	2,7188391	25,002040	2,7410335
14:53	25,002040	2,9555816	24,997154	2,7743256
15:04	25,002040	2,8852987	24,967826	2,6670517
15:15	25,002040	3,0295634	25,002040	2,8039183
15:25	25,002040	2,9592807	25,002040	2,6818482
15:36	25,002040	2,9629797	25,002040	2,6411581
15:49	25,002040	2,6855471	24,997154	2,4562027
16:03	25,002040	2,8150157	25,002040	2,3304331
16:14	25,002040	2,7669274	25,002040	2,2083625
16:24	25,002040	2,6485562	25,002040	2,0825934
16:35	25,002040	2,5782732	25,002040	1,9309303
16:46	25,002040	2,5523793	25,002040	1,8421522
16:58	25,002040	2,2379553	25,002040	1,6387012
17:13	25,002040	2,2675483	25,002040	1,4537465
17:24	25,002040	2,1380794	25,002040	1,2983844
17:34	25,002040	1,9975141	25,002040	1,1097300
17:45	25,002040	1,8717447	25,002040	0,9654651
17:58	25,002040	1,6460994	24,981267	0,7435192
18:11	25,002040	1,1985085	24,703870	0,5363695
18:26	25,002040	0,6473426	23,404888	0,2626361
18:37	22,349084	0,1701586	20,880247	0,1442649
18:48	19,253765	0,0702829	16,975965	0,0776811
The average	**24,690612**	**2,3389275**	**24,471830**	**1,9340816**

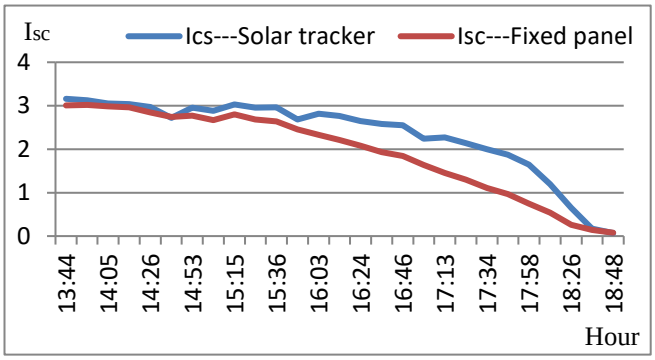

Fig. 34. A graphical comparison of the results of the experiment of January 27, 2022.

8. Discussion

We know that the short circuit current Isc is proportional to solar radiation. We will compare the daily average of Isc provided by the two systems (fixed panel and moving panel).

The daily average of the Isc current provided by the panel in tracking mode is 2.34 A, while that of the panel in fixed mode is 1.93 A. This means that with the panel in tracking mode, we have a gain of about 21.24% compared to that in stationary mode.

The experiment was done during the winter (January 27), which explains the lower gain compared to other studies. According to equation (1), on the day of the experiment on January 27, the sun will have a solar declination angle (δ) equal to -19°, and according to the simulation study of our research published in 2021 [20], (simulation which uses the same characteristics as the equatorial solar tracker used in the experiment), the solar radiation gain of a panel in tracking mode is 27.15% compared to a panel in fixed mode, which leads us to conclude that the results are almost similar, knowing that the simulation is made with solar radiation. This simulation [20] also tells us that the follower model will have a maximum gain of 63.47% between June 21 and July 06 (the sun at this time will have a declination equal to δ=+23°), which is more important than all the research results cited in the introduction [14, 15, 16].

9. Conclusion

This paper is a proposal for a new tracking method capable of offering remarkable accuracy for solar trackers. Instead of using a solar sensor to specify the position of the sun during tracking, we proposed observing the power supplied by the photovoltaic panel at its output. This power is controlled by an MPPT before it is injected into the grid. The idea is to install between the PV and the MPPT a voltage and current sensor to observe this power. As the tracker rotates, the solar tracker control board observes the power Pmpp. As it increases, the tracker continues to activate the tracking motor. The moment the control board detects the decrease in Pmpp, this means that we are at maximum solar radiation and therefore we are well oriented towards the sun, the tracking engine stops. A simulation showed us the reliability of this method. In order to enhance the proposed method, we introduced it into the control chart of an equatorial solar tracker. Real experiments led us to conclude that the method works well, with a remarkable power gain compared to other studies in the field.

Perspective

The next study will be on an azimuthal tracker with two tracking axes; horizontal and vertical, which means that we will observe the power Pmpp during the movement of the horizontal motor and the vertical motor.

References

[1] A. Kazemian, Arash, A. Taheri, A. Sardarabadi, T. Ma, M. Passandideh, and J. Peng, "Energy, exergy and environmental analysis of glazed and unglazed PVT system integrated with phase change material: An experimental approach", Solar Energy, vol. 201, pp. 178-189, 2020.

[2] Z. Abousserhane, A. Abbou, and H. Bouzakri, "Developed Power Flow Control of PV/Battery/SC Hybrid Storage System Featuring Two Grid Modes", International Journal of Renewable Energy Research (IJRER), vol. 12, no. 1, pp. 190-199, 2022.

[3] Z. Abousserhane, A. Abbou, and H. Bouzakri, "Effective Power Management of PV/Battery Hybrid System Under Varying Frequency Modes", 2nd International Conference on Innovative Research in Applied Science, Engineering and Technology (IRASET), pp. 1-8, 2022.

[4] J. Hu, and T. Yachi, "Photovoltaic Systems with Solar Tracking Mirrors", 2nd International Conference on Renewable Energy Research and Applications, Madrid, pp. 201-204, 20-23 October 2013.

[5] H. Bouzakri, A. Abbou, and K. Chennoufi, "Efficiency Enhancement of a Fixed Photovoltaic Panel Using Simple Motorized Reflection Model", vol. 14, no. 4, pp. 77-90, 2021.

[6] A. Al-Ghasem, G. Tashtoush, and M. Aladeemy, "Experimental Study of tracking 2-D Compound Parabolic Concentrator (CPC) with flat plate absorber", 2nd International Conference on Renewable Energy Research and Applications, Madrid, pp. 779-782, 20-23 October 2013.

[7] A. A. Awasthi, A. K. Shukla, M. Manohar S.R. , C. Dondariya, K.N. Shukla, D. Porwal, and G. Richhariya, "Review on sun tracking technology in solar PV system", Energy Reports, vol. 6, pp. 392-405, 2020.

[8] J. F. Alvarado-M, E. Betancur, and A. Velásquez-Lopez, "Optimization of Single-Axis Discrete Solar Tracking", 10th International Conference on Renewable Energy

Research and Application (ICRERA), IEEE, pp. 271-275, 2020.

[9] A. K. Saymbetov, M. K. Nurgaliyev, Ye. Tulkibaiuly, Yo. K. Toshmurodov, Ye. D. Nalibayev, G. B. Dosymbetova, N. B. Kuttybay, M. M. Gylymzhanova, and Ye. A. Svanbayev, "Method for Increasing the Efficiency of a Biaxial Solar Tracker with Exact Solar Orientation", Applied Solar Energy, vol. 54, no. 2, pp. 126-130, 2018.

[10] E. K. Mpodi, Z. Tjiparuro, and O. Matsebe, "Review of dual axis solar tracking and development of its functional model", Procedia Manufacturing, vol. 35, pp. 580-588, 2019.

[11] N. Tiwari, R. Soni, A. Saraswat, and B. Kumar, "Comparative Simulation Study of Dual-Axis Solar Tracking System on Simulink Platform", Intelligent Computing Techniques for Smart Energy Systems. Springer, Singapore, pp. 359-365, 2019.

[12] Y. Yao, Y. Hu, S. Gao, G. Yand, and J. Du, "A multipurpose dual-axis solar tracker with two tracking strategies", Renewable Energy, Vol. 72, pp. 88-98, 2014.

[13] S. J. Oh, M. Burhan, K. C. Ng, Y. Kim, and W. Chun, "Development and performance analysis of a two-axis solar tracker for concentrated photovoltaics", International Journal of Energy Research, vol. 39, no 7, pp. 965-976, 2015.

[14] C. Jamroen, P. Komkum, S. Kohsri, W. Himananto, S. Panupintu, and S. Unkat, "A low-cost dual-axis solar tracking system based on digital logic design: Design and implementation", Sustainable Energy Technologies and Assessments, vol. 37, pp. 100618, 2020.

[15] Z. El Jaouhari, Y. Zaz, S. Moughyt, O. El Kadmiri, and Z. El Kadmiri, "Dual-axis solar tracker design based on a digital hemispherical imager", Journal of Solar Energy Engineering, vol. 141, no. 1, 2019.

[16] H. Fathabadi, "Novel high efficient offline sensorless dual-axis solar tracker for using in photovoltaic systems and solar concentrators", Renewable Energy, vol. 95, pp. 485-494, 2016.

[17] H. Bouzakri, and A. Abbou, "Study and realization of a monoaxial solar tracker over an equatorial mount", 7th International Renewable and Sustainable Energy Conference (IRSEC), pp. 1-6, 2019.

[18] H. Bouzakri, and A. Abbou, "Mono-axial solar tracker with equatorial mount, for an improved model of a photovoltaic panel", International Journal of Renewable Energy Research (IJRER), vol. 10, no 2, pp. 578-590, 2020.

[19] H. Bouzakri, A. Abbou, and Z. Abousserhane, "Model for maximizing fixed photovoltaic panel efficiency without the need to change the tilt angle of monthly or seasonal frequency", 2nd International Conference on Innovative Research in Applied Science, Engineering and Technology (IRASET), IEEE, pp. 1-5, 2022.

[20] H. Bouzakri, A. Abbou, K. Tijani, and Z. Abousserhane, "Biaxial Equatorial Solar Tracker with High Precision and Low Consumption: Modelling and Realization", International Journal of Photoenergy, vol. 2021.

[21] M. Iqbal, An Introduction to Solar Radiation, Elsevier, 1983.

[22] R. EL idrissi, A. Abbou, M. Mokhlis, H. Bouzakri, and Y. El houm, "Real- Time implementation of a PV system maximum power point tracking based on the ANN-Backstepping sliding mode control", International Journal of Renewable Energy Research, vol 11, no. 4, pp. 1959-1967, 2021.

[23] K Chennoufi, and M Ferfra, "Fast and efficient Maximum Power Point Tracking controller for photovoltaic modules", Advances in Science, Technology and Engineering Systems Journal, vol. 5, no. 6, pp. 606-612, 2020.

[24] A. F. Alsulami, and S. M. S. AL Arefi, "Fraction Open Circuit and Fractional Short Circuit Based Incremental Conductance Maximum Power Point Tracking Controller", 10th International Conference on Renewable Energy Research and Application (ICRERA), IEEE, pp. 184-189, 2021.

[25] C. Aoughlis, A. Belkaid, I. Colak, O. Guenounou, and M. A. Kacimi, "Automatic and Self Adaptive P&O MPPT Based PID Controller and PSO Algorithm", 10th International Conference on Renewable Energy Research and Application (ICRERA), IEEE, pp. 385-390, 2021.